Ke Ai

Contents lists available at ScienceDirect

Bioactive Materials

journal homepage: http://www.keaipublishing.com/biomat



In vitro degradation and biocompatibility evaluation of typical biodegradable metals (Mg/Zn/Fe) for the application of tracheobronchial stenosis



Yangyang Li^a, Jianglong Yan^a, Wenhao Zhou^a, Pan Xiong^a, Pei Wang^a, Wei Yuan^b, Yufeng Zheng^b, Yan Cheng^{a,*}

- ^a Academy for Advanced Interdisciplinary Studies, Peking University, Beijing, 100871, China
- ^b Department of Materials Science and Engineering, College of Engineering, Peking University, Beijing, 100871, China

ARTICLE INFO

Keywords: Biomaterials Biodegradable metals Corrosion Tracheobronchial stents Cytocompatibility

ABSTRACT

Tracheobronchial obstruction in children due to benign stenosis or tracheobronchomalacia still remains a challenging matter of concern. Currently, there is 10%–20% complication rate in clinical treatment. The non-biodegradable property of silicone stents and nickel-titanium memory alloy stents take the primary responsibility for drawbacks including stimulating local granulation tissue proliferation, displacement, and stent-related infections. Permanent tracheobronchial stent will be a persistent foreign object for a long time, causing excessive secretion of tracheal mucosa, ulceration and even perforation, which is particularly unsuitable for young children with persistent tracheal growth. In this study, the degradation and biocompatibility performance of three typical biodegradable metals were investigated as potential tracheobronchial stent materials. The results exhibited that these materials showed different degradation behaviors in the simulating respiratory fluid environment compared with SBF. Except for pure iron group, high purity magnesium and zinc showed favorable cell adhesion and proliferation in three culture methodologies (direct culture, indirect culture and extraction culture). The proper corrosion rate and good biocompatibility indicated that high purity magnesium and zinc may be good candidates as tracheobronchial stent materials.

1. Introduction

Tracheal stenosis in newborns and small infants often causes multiple complications and high mortality. With the features of undeveloped muscles and easily deformed walls, the postoperative airway tissue is difficult to heal for children [1]. Regrettably, at present, there is no clinically dedicated stent for the tracheobronchial construction in children, and only stents following the trail of the experience in adult group can be used. And there is no need to place the stent in infant child for the lifetime. It's enough to provide a necessary support during the first 3–12 months, then a second surgery is required to allow the growth and development of the airway tissue [1,2]. However, complications about insufficient mechanical properties and granulation tissue hyperplasia about undegradable intravascular stents are reported after implantation in children's airways [2].

As experience, some biodegradable materials for airway stents have been studied. For example, biodegradable polydioxanone (PDS) selfexpanding stents could maintain clinical improvement for 43 months in the airway of children [3]. Especially, biodegradable metal such as magnesium, zinc and iron have been identified as the promising candidates for biodegradable medical device due to their superior biocompatibility and mechanical property. The magnesium and ion vascular stents have been stepping into clinical stage [4,5]. A tracheal stent made by magnesium alloys persisted during the implantation in a rat tracheal model for 6 months [6]. However, there are few studies in vitro that focus on comparing the performance of these biodegradable metal in tracheobronchial environment. It is necessary to systematically identify the different degradation and biocompatibility performance of biodegradable metal before their clinic application.

In this study, the degradation and biocompatibility behaviors of high purity magnesium, zinc and iron in airway environment were studied. The biodegradable metal was immersed in Gamble's solution (GS) simulating the respiratory fluid environment for 4 weeks, and SBF solution was as control. Particularly, three different cell culture

Peer review under responsibility of KeAi Communications Co., Ltd.

E-mail address: chengyan@pku.edu.cn (Y. Cheng).

^{*} Corresponding author.

Table 1
Composition and pH of simulated physiological media discussed in this study.

Chemical	Content(g/L)	
	GS	SBF
$MgCl_2$	0.095	0.146
NaCl	6.019	8.035
KCl	0.298	0.225
Na ₂ HPO ₄	0.126	-
K₂HPO₄·3H₂O	_	0.231
Na ₂ SO ₄	0.063	0.072
CaCl ₂	0.278	0.292
CH ₃ COONa	0.574	-
NaHCO ₃	2.604	0.355
C ₆ H ₅ Na ₃ O ₇ ·2H ₂ O	0.097	-
Porcine stomach mucin	0.6	-
Tris (HOCH ₂) ₃ CNH ₂	_	6.118
pH	7.35	7.3–7.4

methodologies were designed to mimic the environment around tracheobronchial stent in vivo closely. The in vitro degradation behavior and cytocompatibility were characterized, which may provide guidance for further application of high purity magnesium, zinc and iron as tracheobronchial stent.

2. Materials and methods

High purity magnesium (HP-Mg; 99.99%), high purity zinc (HP-Zn; 99.999%), and pure iron(P-Fe; 99.9%) for microstructure characterization, electrochemical testing and in vitro cell culture were cut into disks (\emptyset 10 × 2mm), polished by SiC abrasive paper up to 2000 grit.

GS and SBF solution were prepared by previous study [7], and the solution composition was listed in Table 1. According to ASTM F3268-18, static immersion test was carried out in 37°C, and the ratio of solution volume to sample area was 20 mL/cm². The pH value was recorded at each time point. At 7, 14, 21 and 28 days, the samples were collected from GS and SBF solution. The corrosion products were characterized by FTIR (Spotlight 200, PerkinElmer), Changes on surface morphologies were observed with SEM (Quanta 200FEG) coupled with EDS. After immersion for different time, the samples (n = 3) were immersed into 200 g/L CrO₃ solution for about 10 min, and this process was repeated several times until removing all the corrosion products [8]. Then the dry samples were weighed to calculate the corrosion rate. For electrochemical test, potentiodynamic polarization (PDP) curves were acquired by using a three-electrode cell configuration with a platinum plate as counter electrode and a saturated calomel electrode as reference electrode. The human lung adenocarcinoma type-II alveolar epithelial cells A549 were cultured in McCoy's 5A Media with

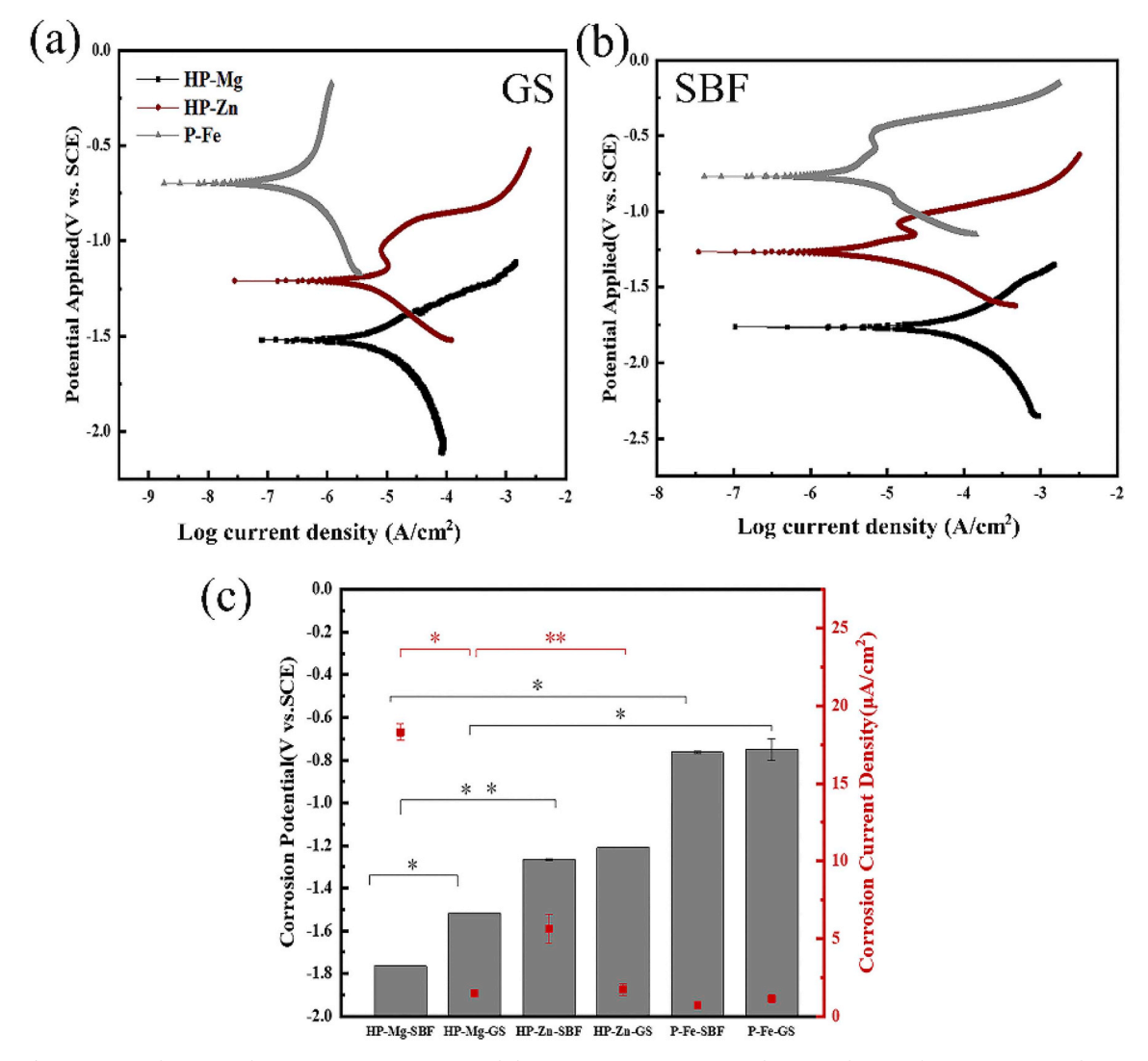


Fig. 1. Potentiodynamic polarization curves in (a) GS and (b) SBF; (c) Corrosion potential/current density of HP-Mg, HP-Zn and P-Fe.

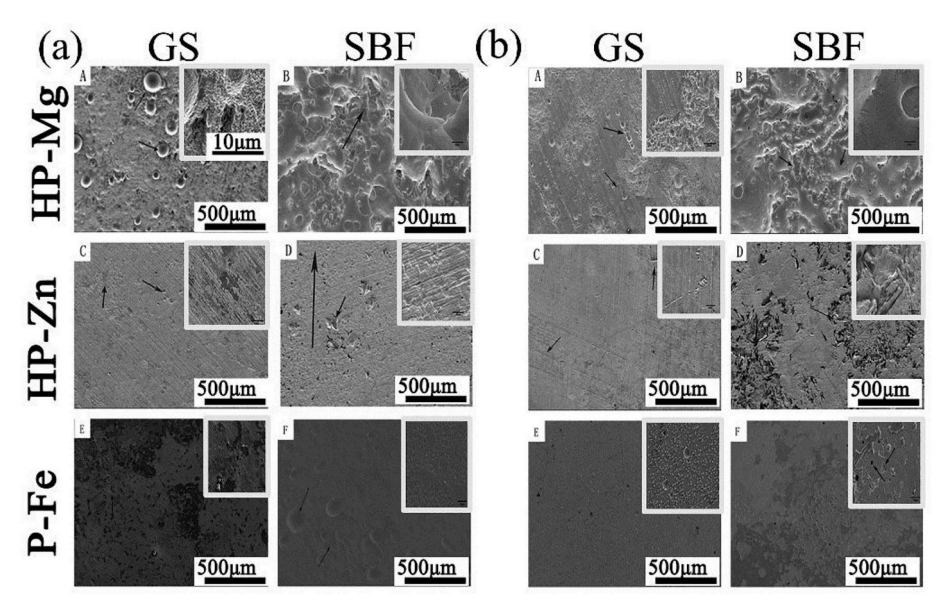


Fig. 2. SEM image of corrosion surface on (a) 7 d and (b) 14 d.

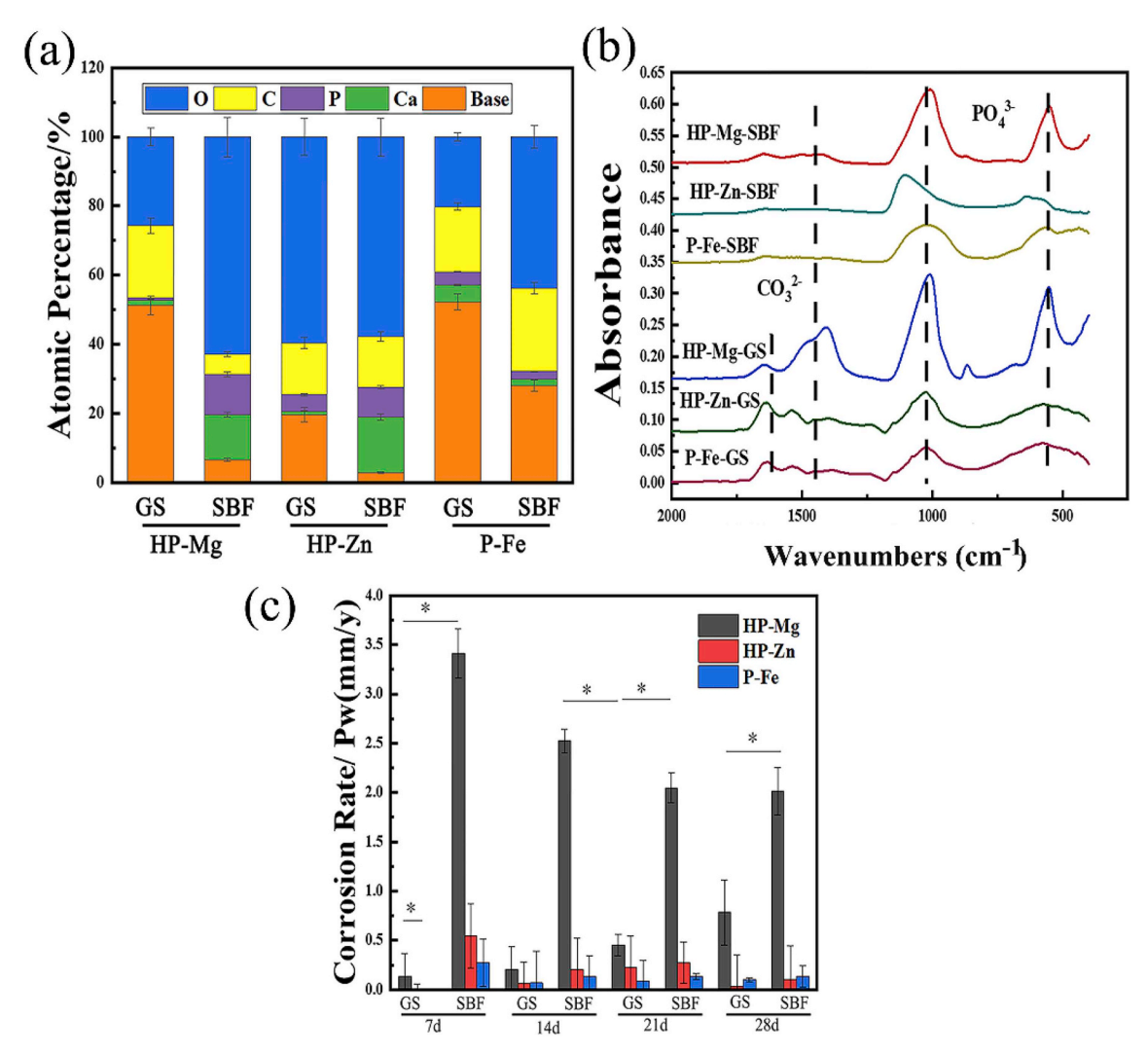


Fig. 3. (a) Atomic percentage of corrosion products and (b) FTIR transmission spectra of the corrosion products after 7-day-immersion period; (c) Corrosion rate during 4-week-immersion period.

Table 2The difference in composition concentration between GS and SBF solution.

Chemical Component	Content	
	GS	SBF
C1-	114.0 mM	147.8 mM
HCO ₃	30.8 mM	4.2 mM
Protein	$0.6\mathrm{g/L}$	-

10% FBS under 37 °C. As shown in Fig. 6(a), three different methodologies of cell culture including direct culture (DC), indirect culture (IC) and extraction culture (EC) were prepared to simulate different growth environment of cells with the tracheobronchial stent in vivo by previous study [9]. After 1, 3 and 5 days, Cell Counting Kit-8 (CCK-8, Dojindo Molecular Technologies, Japan) was used to value the cell viability at a single wavelength of 450 nm with a microplate reader. At 48 h and 96 h, the cell morphology was evaluated with SEM or Laser Scanning Confocal Microscope (LSCM; A1R-si, Nikon). Additionally, an Inductively Coupled Plasma Optical Emission Spectroscope (ICP-OES, iCAP6300, Thermo) was used to determine the ion concentrations in the gathered extracts in EC culture medium.

3. Results and discussion

Fig. 1 summarized the electrochemical results obtained from the electrochemical tests in GS or SBF. By the PDP curves (Fig. 1(a) and

(b)), for HP-Zn and P-Fe, no significant differences in statistical results of corrosion potential value and corrosion current density for samples immersed in GS and SBF. In contrast, higher cathodic corrosion potential value and lower corrosion current density (Fig. 1(c)) were observed for HP-Mg immersed in GS than in SBF, indicting the GS electrolyte solution had more moderate corrosion property for HP-Mg. Hence, it is vital to control the degradation rate of pure Mg and its alloys for safe biomedical deployments. Extensive effort including microstructural and surface modification strategies has been devoted to address the corrosion issue of Mg alloys [10–12].

The corrosion topography of the samples immersed for 2 weeks were observed by SEM, and shown in Fig. 2. On the 7 d, for samples immersed in GS, the most severe corrosion happened in HP-Mg (Fig. 2(a)A), which started at discrete sites, and expanded to cover the whole specimen on 14 d (Fig. 2(b)A). The corrosion of HP-Mg immersed in SBF even got worse with nearly complete corroded surface on 7 d (Fig. 2(a)B). Inversely, the corrosion area on HP-Zn and P-Fe was still at discrete sites even on 14 d in SBF (Fig. 2(b)D and Fig. 2(b)F). After 7day-immersion period, the corrosion products on the samples surface were detected by EDS and FTIR (Fig. 3(a) and (b)). The FTIR results (Fig. 3(b)) showed that most of the corrosion products were carbonate and phosphate, which provided protective layer for samples immersed in both GS and SBF [13-15]. However, for HP-Mg and HP-Zn immersed in GS, less phosphate products were detected compared with same samples immersed in SBF (Fig. 3(a)). It was determined that protein like porcine stomach mucin was co-precipitated with phosphate and had a strong negative effect on the precipitation of phosphates [16]. And the calculated corrosion rates after 28-day immersion (Fig. 3(c)) in GS were

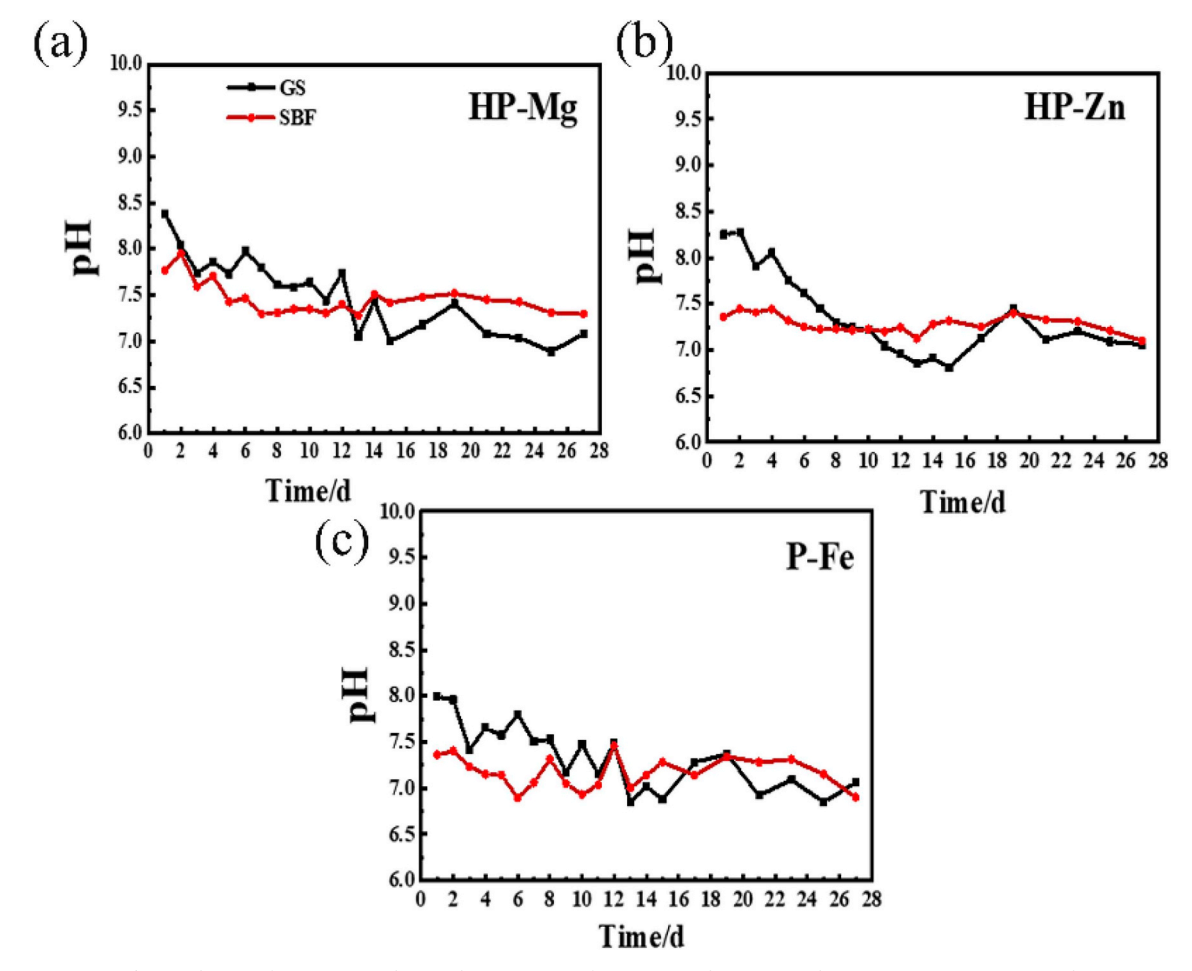


Fig. 4. The pH of immersion solution change curves of (a) HP-Mg, (b) HP-Zn and (c) P-Fe in immersion period.

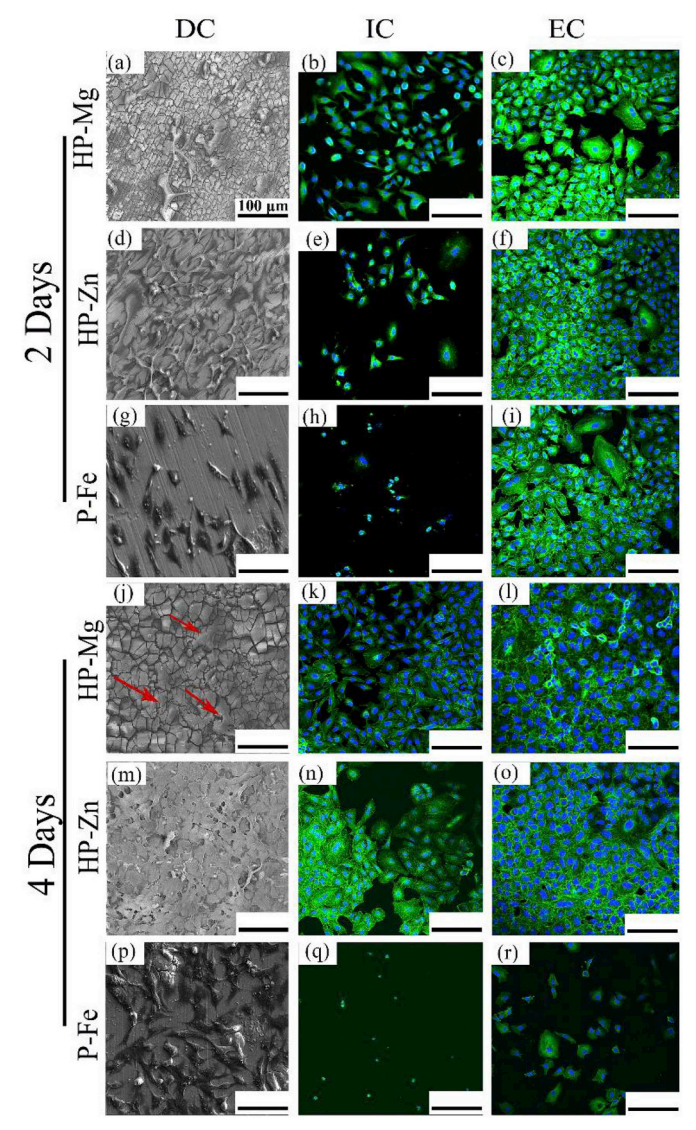


Fig. 5. SEM and fluorescence images of A549 under different cell culture conditions.

only 0.78 mm/y, 0.034 mm/y and 0.102 mm/y for HP-Mg, HP-Zn and P-Fe, respectively, which were lower than SBF group (2.01 mm/y in HP-Mg, 0.102 mm/y in HP-Zn and 0.136 mm/y in P-Fe). As shown in Table 2, the concentration of chloride and bicarbonate in SBF was nearly 1.3 times and 7.3 times than that in GS, respectively. Additionally, protein with concentration of 0.6 g/L was added to GS. The difference in composition concentration between GS and SBF solution was the main reason for above results. By the reaction between bicarbonate and hydroxide and protein adsorption, the metal immersed in aqueous solution with the formation of insoluble protective layer show more tardy corrosion rate [15,17]. However, the protective film on metal surface is easily broken down by the dissolved chloride salts and pitting corrosion was caused [13]. Therefore, with lower concentration of chloride and higher concentration of bicarbonate and protein in GS, the corrosive effects caused by GS seem to be less serious than SBF. Overall, as for the degradation behaviors, compared with SBF, pH change in GS was less constant and stable (Fig. 4(a)-(c)). The different contents in buffer (HCO₃⁻/CO₂ in GS vs. Tris/HCl in SBF) were responsible for that. The pH buffers such as Tris or CO2 can influence the metal degradation which yield different degradation performance [18]. GS showed poor buffering capacity in this study. The decreased pH value may be due to low CO_2 concentration in GS solution since there lacked active pH control setup to feed gaseous CO_2 into the testing medium. Schinhammer et al. [18] designed a CO_2 -controller setup to feed gaseous CO_2 into the testing solution and actively regulate the pH value, which kept the pH value in the range between 7.35 and 7.45.

Fig. 5 showed A549 cells behaviors under three different culture methodologies. When comparing with the same substrate, the DC and EC group showed much higher cell density than IC group at day 2 and day 4, where cells were in typical epithelioid and polygonal shapes, and displayed better adhesion. In DC and EC group, the difference in A549 cells density between HP-Mg and HP-Zn was not statistically significant at day 2 and day 4. But cell density in P-Fe showed an obvious reduction at day 4 in EC group. However, previous study [19] revealed that Fe-based stents stimulated the proliferation of L929 and ECV304 cells. And the performance of P-Fe with A549 cells under EC situation needs further study. The cytotoxicity test (Fig. 6(b)) revealed that at day 1, P-Fe-IC had the strongest cytotoxicity compared with the negative group. The following 2 days witnessed an obvious increase for HP-Mg-EC and HP-Zn-EC. And at day 5, all the HP-Mg group, HP-Zn-DC and HP-Zn-IC ended with similar viability values with negative group. This might attribute to the difference among cell culture methodologies as more deposition of corrosion productions on substrates surface in DC group provided a protection layer. As for the difference between cell morphology (Fig. 5(j)) and cytotoxicity test results (Fig. 6(b)) for HP-Mg in DC group, the cells on the bottom of the culture plates may be the main reason to cause higher absorbance value. Additionally, ICP results (Fig. 6(c)) exhibited ions concentration in EC culture medium. 0.23 mM Zn^{2^+} group and 6.03 mM Mg $^{2^+}$ group showed no obvious cytotoxicity on A549 cells, whereas, cytotoxicity of 1.52 mM Fe²⁺/Fe³⁺ group was visible. In summary, compared with P-Fe, HP-Mg and HP-Zn showed better cell adhesion and proliferation behaviors.

4. Conclusions

The present study investigated the potential application of HP-Mg, HP-Zn and P-Fe as stents in tracheobronchial obstruction of children. Compared with samples immersed in SBF, samples immersed in GS showed much slower corrosion rate. Furthermore, in term of cell viability and cellular morphology, no obvious cytotoxicity was observed in the HP-Mg and HP-Zn groups, they showed better cell adhesion and proliferation behaviors when comparing to P-Fe. Consequently, HP-Mg and HP-Zn with proper corrosion rate and good biocompatibility shows a great potential for developing biodegradable tracheobronchial stents.

Conflict of interest statement

We declare that we have no financial and personal relationships with other people or organizations that can inappropriately influence our work, there is no professional or other personal interest of any nature or kind in any product, service and/or company that could be construed as influencing the position presented in, or the review of, the manuscript entitled, "In vitro degradation and biocompatibility evaluation of typical biodegradable metals (Mg/Zn/Fe) for the application of tracheobronchial stenosis".

Acknowledgements

This work is jointly supported by National Natural Science Foundation of China (No. 31670974, No. 31370954).

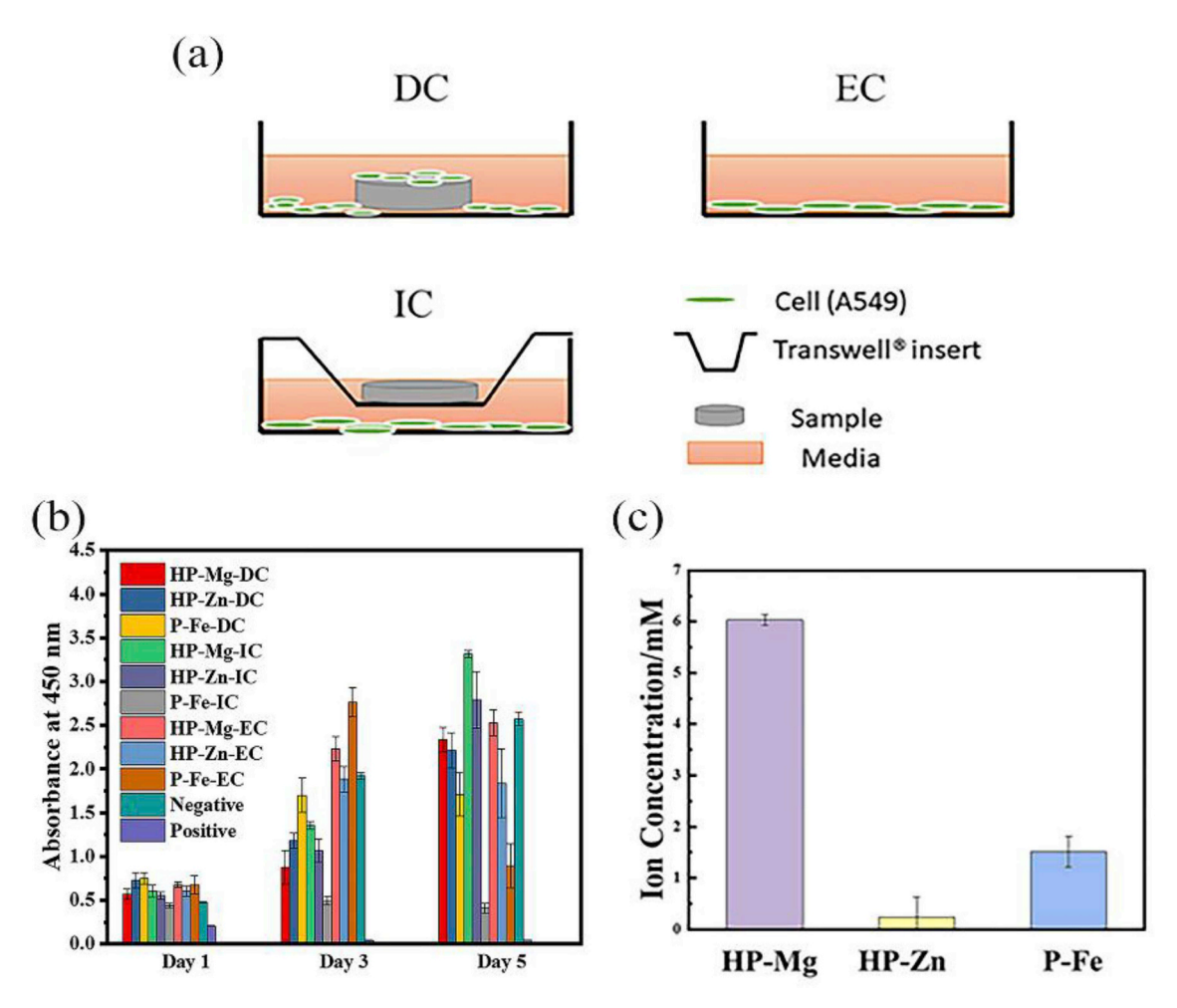


Fig. 6. (a) Illustrations of different cell culture methodologies: direct culture (DC), indirect culture (IC), and extraction culture (EC); (b) CCK-8 assay of A549 and (c) ion concentration in EC medium.

References

- J.Z. Tan, M. Ditchfield, N. Freezer, Tracheobronchomalacia in children: review of diagnosis and definition, Pediatr. Radiol. 42 (2012) 906–915.
- [2] J.L. Anton-Pacheco, Tracheobronchial stents in children, Semin. Pediatr. Surg. 25 (2016) 179–185.
- [3] J.L. Antón-Pacheco, C. Luna, E. García, et al., Initial experience with a new biodegradable airway stent in children: is this the stent we were waiting for? Pediatr. Pulmonol. 51 (2016) 607–612.
- [4] A. Francis, Y. Yang, S. Virtanen, A.R. Boccaccini, Iron and iron-based alloys for temporary cardiovascular applications, J. Mater. Sci. Mater. Med. 26 (2015) 138.
- [5] R. Erbel, C. Di Mario, J. Bartunek, J. Bonnier, B. de Bruyne, F.R. Eberli, P. Erne, M. Haude, B. Heublein, M. Horrigan, C. Ilsley, D. Böse, J. Koolen, T.F. Lüscher, N. Weissman, R. Waksman, Temporary scaffolding of coronary arteries with bioabsorbable magnesium stents: a prospective, non-randomised multicentre trial, Lancet 369 (2007) 1869–1875.
- [6] L. Sarah, Magnesium Alloys for Use as an Intraluminal Tracheal Stent, Master's Thesis University of Pittsburgh, 2013, http://d-scholarship.pitt.edu/18436/.
- [7] M.R.C. Marques, R. Loebenberg, M. Almukainzi, Simulated biological fluids with possible application in dissolution testing, Dissolution Technol. 18 (2011) 15–28.
- [8] D.M. Brasher, J.G. Beynon, K.S. Rajagopalan, J.G.N. Thomas, Passivity of iron in chromic acid solutions, Br. Corros. J. 5 (2013) 264–269.
- [9] Q. Tian, M. Deo, L. Rivera-Castaneda, H. Liu, Cytocompatibility of magnesium alloys with human urothelial cells: a comparison of three culture methodologies, ACS Biomater. Sci. Eng. 2 (2016) 1559–1571.
- [10] L.-Y. Li, L.-Y. Cui, R.-C. Zeng, S.-Q. Li, X.-B. Chen, Y. Zheng, M.B. Kannan, Advances

- in functionalized polymer coatings on biodegradable magnesium alloys a review, Acta Biomater. 79 (2018) 23–36.
- [11] M.-S. Song, R.-C. Zeng, Y.-F. Ding, R.W. Li, M. Easton, I. Cole, N. Birbilis, X.-B. Chen, Recent advances in biodegradation controls over Mg alloys for bone fracture management: a review, J. Mater. Sci. Technol. 35 (2019) 535–544.
- [12] L.C. Rongchang ZENG, K.E. Wei, Biomedical magnesium alloys: composition, microstructure and corrosion, Acta Metall. 54 (2018) 1215–1235.
- [13] G. Song, A. Atrens, Understanding magnesium corrosion—a framework for improved alloy performance, Adv. Eng. Mater. 5 (2003) 837–858.
- [14] Z. Li, G.-L. Song, S. Song, Effect of bicarbonate on biodegradation behaviour of pure magnesium in a simulated body fluid, Electrochim. Acta 115 (2014) 56–65.
- [15] V. Wagener, A.S. Faltz, M.S. Killian, P. Schmuki, S. Virtanen, Protein interactions with corroding metal surfaces: comparison of Mg and Fe, Faraday Discuss 180 (2015) 347–360.
- [16] Y. Jang, D. Owuor, J.T. Waterman, L. White, B. Collins, J. Sankar, T.W. Gilbert, Y. Yun, Effect of mucin and bicarbonate ion on corrosion behavior of AZ31 magnesium alloy for airway stents, Materials (Basel) 7 (2014) 5866–5882.
- [17] S. Virtanen, Biodegradable Mg and Mg alloys: corrosion and biocompatibility, Mater. Sci. Eng., B 176 (2011) 1600–1608.
- [18] M. Schinhammer, J. Hofstetter, C. Wegmann, F. Moszner, J.F. Löffler, P.J. Uggowitzer, On the immersion testing of degradable implant materials in simulated body fluid: active pH regulation using CO₂, Adv. Eng. Mater. 15 (2013) 434–441
- [19] Y.F. Zheng, X.N. Gu, F. Witte, Biodegradable metals, Mat. Sci. Eng. R 77 (2014) 1–34.